Title: A study on utilization of stainless steel wire cloth as a catalyst support

Authors: Ki-Joong Kim, Ho-Geun Ahn

PII: S1226-086X(11)00246-2
DOI: doi:10.1016/j.jiec.2011.11.061
Reference: JIEC 701

To appear in:

Received date: 5-5-2011
Accepted date: 25-6-2011

Please cite this article as: K.-J. Kim, H.-G. Ahn, A study on utilization of stainless steel wire cloth as a catalyst support, *Journal of Industrial and Engineering Chemistry* (2010), doi:10.1016/j.jiec.2011.11.061

A study on utilization of stainless steel wire cloth as a catalyst support

Ki-Joong Kim[a], Ho-Geun Ahn[b,*]

[a]*School of Chemical, Biological & Environmental Engineering, Oregon State University, Corvallis, Oregon 97331, USA*

[b]*Department of Chemical Engineering, Sunchon National University, 315 Maegok, Suncheon, Jeonnam 540-742, South Korea*

* Corresponding author. Tel.: +82 61 750 3583.

E-mail address: hgahn@sunchon.ac.kr (H.-G. Ahn).

ABSTRACT

In this work, stainless steel wire cloth (SSWC) for metallic support was thermally treated to increase the adhesive strength of Al_2O_3 by improving superficial roughness. After coating Al_2O_3 on SSWC, Pt particles as a catalytic component were deposited on the Al_2O_3/SSWC. These supports and catalysts were characterized by N_2 gas adsorption, X-ray diffraction (XRD), scanning electron microscopy (SEM) in conjunction with energy dispersive spectroscopy (EDS), and scanning transmission electron microscopy (STEM). The catalytic performance was tested in the ethylene oxidation. The effect of space velocity (GHSV = 2,000 - 8,000 h^{-1}) at different temperatures (190 ℃ and 210 ℃) and reproducibility were investigated. The superficial roughness of SSWC was markedly increased by thermal oxidation at 800 ℃ for 12 h, and good adherence of Al_2O_3 to the SSWC was observed. The obtained Pt/Al_2O_3/SSWC800 catalyst showed excellent catalytic activity in the ethylene oxidation and showed a good reproducibility and stability even after repeated use.

Keywords*: Metallic support; Thermal treatment; SEM; Ethylene oxidation*

1. Introduction

For pollution abatement applications it is common to utilize a monolithic honeycomb structured catalyst to minimize the pressure drop associated with high flow rates [1,2]. The honeycomb is usually inside a steel housing and physically fixed in the exhaust. This allows the process effluent gases to pass uniformly through the channels of the honeycomb. Monolithic honeycomb materials offer a number of advantages over more traditional pellet-shaped catalysts and, thus, are widely used as supports in environmental applications [3]. The preparation of monolithic catalysts consists of the two-step process: mainly, the deposition of the oxide layer (or primer) with high surface area on the channel walls because it has large pores and low surface area, and deposition of the active metal on the oxide layer. This is referred to as the wash-coat. Generally, the most commonly used primer is γ-Al_2O_3 due to the chemical, hydrothermal, and mechanical stability in order to improve surface areas [4]. In these processes, the main problems are obtaining homogeneity with a good adhesion of the oxide layer and achieving high dispersion of the active metal on that oxide layer.

Monolithic supports are typically made of either ceramics or metals. Ceramic supports have been widely used due to the ease of the deposition of the active metal. They have been used as a support for controlling emissions of air pollutants in exhaust gases, e.g. selective catalytic reduction of NOx, combustion of VOCs, and three way catalysts [5,6], but have some drawbacks as well: the low heat-transfer rate and the high price [7]. Recently, much attention was paid to the practical use of metallic supports such as stainless steel [8-10,14-23] and aluminum [11-13]. The main advantages of metallic supports, particular stainless steel, compared with ceramic support can be summarized as follows: high anticorrosion, high mechanical strength, high thermal conductively, endurance, and lower cost [8-23]. However, the metallic supports could not be applied in practice because of a low adherence of the primer to the metallic support. The coefficient of thermal expansion of the metallic support is different from the oxide layer, so a suitable pretreatment method for the metallic substrate is required in order to improve the primer adherence.

Many different methods have been proposed for improving adherence, such as wet oxidation by acid [8-11], anodic oxidation [12-14], and thermal oxidation [15-23], especially thermal oxidation at high temperature has been considered because it requires a simple apparatus. These metallic supports just used in lab scale processes include the hydrogenation of acetophenone [8],

photo-catalytic decomposition of ammonia [10], Fisher-Tropsch process [11], CO oxidation [13,15-17], partial oxidation of methane [18], selective catalytic reduction of NOx [17,19], and decomposition of VOCs [9,12,14,20,21]. Also, catalytic activity depended strongly upon the shape of support, which may relate to mass/heat transfer rates and contact time with reactant gas in the higher space velocity system. Although plate shape [10,14] and cylinder shape [11-13,15-23] were examined, mesh shaped metallic support [8,9,24] has a good mass/heat transfer performance as well as low pressure drop during the higher space velocity, therefore exhibiting a higher activity than the ceramic honeycomb.

In this work, first stainless steel wire cloth (SSWC) for metallic support was thermally treated to increase the adhesive strength of Al_2O_3 as a primer by improving superficial roughness. After wash-coat of Al_2O_3, highly dispersed active metal, Pt was deposited. Catalytic performances for ethylene oxidation over Pt/Al_2O_3 supported on thermally treated SSWC were investigated for potential use as an environmental catalyst system.

2. Experimental

2.1. Preparation of catalysts

Commercial 304 stainless steel wire cloth (SSWC, 40 mesh, wire diameter: 0.18 mm) was used as a raw material. The 304 SSWC was mainly composed of Cr (18.2wt%), Ni (8.6wt%), and Mn (1.5wt%) in Fe balance. SSWC was cut to the size of 0.9 cm×11.5 cm (1.44 g) as needed, and then cleaned in an acetone solution for 0.5 h with an ultrasonic cleaner.

In a previous work, SSWC was pretreated by thermal oxidation, and the optimal surface roughness was achieved at 800 ℃ for 12 h [25]. Before wash-coat of Al_2O_3, SSWC was pretreated by thermal oxidation at 800 ℃ for 12 h in static air atmosphere (SSWC800). The SSWC800 was immersed into the aqueous solution of $Al(NO_3)_3 \cdot 9H_2O$ (100 ml, 1.87 M, Junsei) for 0.5 h, and lifted at a constant speed of 3 cm/h, followed by maintaining at room temperature for 12 h. Then it was dried at 100 ℃ in an oven for 24 h, and calcined at 500 ℃ for 5 h in static air. Hereafter, Al_2O_3 coated SSWC800 is named as Al_2O_3/SSWC800. Pt on Al_2O_3/SSWC800 (Pt/Al_2O_3/SSWC800) was prepared by an impregnation method as follows. Al_2O_3/SSWC800 was put into 100 mL of distilled water, and then an aqueous solution of $H_2PtCl_6 \cdot 5H_2O$ (7 ml,

1.35 x 10^{-3} M, Kojima) was added slowly dropwise with continuous stirring at room temperature, followed by maintaining at room temperature for 12 h. After drawing SSWC out, it was dried at 100 ℃ in oven for 24 h, and calcined at 500 ℃ for 5 h in static air. The Pt/Al_2O_3/SSWC800 was compared with the powdered Pt/Al_2O_3 catalyst. The Pt/Al_2O_3 catalyst was prepared by conventional impregnation method [26], and that has about 4.3wt% of Pt loading content.

2.2. Characterization

The BET surface area, total pore volume and average pore diameter were measured using N_2 gas adsorption analyzer (ASAP 2010, Micromeritics) at -196 ℃. Before the analysis, the sample was pretreated with helium at 200 ℃ for 2 h. The BET surface areas were computed using the BET equation from the amount of N_2 physisorbed at different relative pressures (P/P_0). The total pore volume and average pore diameter were calculated by the Horvath Kawazoe (HK) method. The crystalline phases were identified by X-ray diffraction (XRD, XPERT-PRO, Philips) operating at 40 kV and a current of 30 mA with Cu-Kα_1 radiation (0.154 nm) in the 2θ scan range from 20° to 80° with a step size of 0.04°. The measured XRD patterns were compared with the JCPDS file [27]. The surface morphology was observed by scanning electron microscope (SEM, S4700, Hitachi) using 20-25 kV accelerating voltage. The chemical composition was analyzed by energy dispersive spectroscopy (EDS, Xflash Detector 4010, Bruker AXS). The Pt loading was measured using inductively coupled plasma-atom emission spectrometry (ICP-AES, D-TIME 3000 DC, Perkin Elmer). The sample was digested with a mixture of HNO_3 (70 %) and HCl (35 %) in the ratio of one to three. The Pt particle sizes in the Pt/Al_2O_3/SSWC800 were observed using scanning transmission electron microscopy (STEM, 2010F, Jeol) operating at 200 kV. The Pt/Al_2O_3 layer was raked out from Pt/Al_2O_3/SSWC800, and it was dispersed in ethanol by sonication and dropped on a copper grid with a carbon film. Histograms of the particle size distribution were obtained by counting in the micrographs, and the average particle diameter (*dM*) was calculated using the formula $dM = \Sigma di \cdot ni / \Sigma ni$, where *ni* was the number of particles of diameter *di* [28]. The adherence of the alumina layer on SSWC was tested using the ultrasonic method [29]. The sample was treated in acetone for 1 h at room temperature with ultrasonic cleaner. And then it was dried at 100 ℃ in oven for 12 h, and calcined at 500 ℃ for 3

h in static air atmosphere. Adherence was determined as the ratio of different weight loss before and after the ultrasonic test.

2.3. Activity test

The ethylene oxidation was carried out in a fixed-bed reactor, a rectangular-shape quartz (1 cm x 1 cm x 0.4 cm) reactor packed with 1.5 g of sample. A standard feed gas of 1.0 vol% ethylene in air was passed through the catalyst bed under atmospheric pressure. And the flow rate of reactant gas was controlled to 40 ml/min with mass flow controller. The temperature of the stream line was maintained at 100 ℃ by using a heating band and insulating material. A thermocouple (Al-Cr) was inserted into the catalyst bed to control the reaction temperature. All the samples were pretreated with He flow at 200 ℃ for 1 h before the catalytic test. The conversion of ethylene was determined through the thermal conductivity detector of gas chromatograph (DS-6200, Donam Instrument) with a Porapak Q column (1/8″, 6 ft, ss), and was calculated from the decrease of ethylene detected by the chromatographs. The conversion of ethylene was obtained at steady state (usually 0.5 h after the temperature stabilized), and the experiments were repeated three times to check the reproducibility. The Pt/Al_2O_3/SSWC800 sample was also studied under different gas hourly space velocity (GHSV) in the range of 2,000 - 8,000 h^{-1}, and reproducibility test was performed four times at GHSV = 5,920 h^{-1}. Measurement of catalytic activity using powdered catalyst (Pt/Al_2O_3) to compare to the metallic support was carried out in the same operating conditions. The Pt/Al_2O_3 with 4.3wt% Pt loading is the same Pt loading content as that of the catalytic layer deposited on the metallic support (Al_2O_3/SSWC800). The Pt/Al_2O_3 was packed with glass balls equal to the volume occupied by the metallic support devices.

3. Results and discussion

3.1. Characterization

Textural properties such as BET surface area, total pore volumes and average pore diameters of all the samples were investigated by N_2 gas adsorption, and the results are shown in Table 1. It was observed that the BET surface area of the untreated SSWC used as a raw material was 2.6 ± 0.08 m^2/g, and it was increased by 1.5 times (4.0 ± 0.13 m^2/g) when it was pretreated by thermal

oxidation at 800 ℃ for 12 h. This increased surface area corresponds to an improved surface roughness, which is expected to improve adhesive ability of Al_2O_3 to SSWC surface. BET surface area of Al_2O_3/SSWC800 was markedly increased to 16.9 ± 0.21 m^2/g, and the Pt/Al_2O_3/SSWC800 was 17.0 ± 0.18 m^2/g which is almost the same as Al_2O_3/SSWC800, indicating that the Pt particles have a negligible effect on the textural properties. The total pore volume was increased with increasing BET surface area. The average pore diameter of all samples had similar values, in the range of 2.1 - 2.6 nm. The N_2 adsorption isotherm (Fig. 1) of the Al_2O_3/SSWC800 and Pt/Al_2O_3/SSWC800 shows the typical mesoporous materials, according to the Brunauer-Deming-Deming-Teller classification [30].

The XRD patterns of untreated SSWC (Fig. 2 (a)) shows only the diffraction peaks of the austenitic phase ($2\theta = 43.7^o$, 51.0^o, 74.7^o). The intensity of these peaks for austenitic phase decreases due to the formation of an oxide layer by thermal treatment (Fig. 2 (b)). These new diffraction peaks from the oxide layer can be attributed to martensite ($2\theta = 44.7^o$, 65.3^o), skolaite (Cr_2O_3, $2\theta = 24.5^o$, 33.6^o, 54.6^o), and $Mn_{1+x}Cr_{2-x}O_{4-x}$ ($2\theta = 33.5^o$, 63.0^o), according to JCPDS file [26]. XRD patterns in Fig. 2 (c) confirm that crystalline γ-Al_2O_3 has been deposited on SSWC800 after wash-coat with a aqueous solution of $Al(NO_3)_3{\cdot}9H_2O$ and calcinations. Furthermore, in the case of Pt/Al_2O_3/SSWC800 (Fig. 2 (d)), the major peak (111 plane) of Pt at $2\theta = 39.8^o$ could not be observed due to the overlap with Al_2O_3 of the support, Al_2O_3/SSWC [25].

Fig. 3 shows the SEM images of SSWC, SSWC800, Al_2O_3/SSWC, and Pt/Al_2O_3/SSWC800 samples. Fig. 3 (b) shows clearly that the roughness of the surface was improved by thermal treatment compared to untreated SSWC (Fig. 3 (a)). The generated oxide layer was formed with irregular shaped crystals with diameter ranging from 0.5 to 1 μm. The XRD results suggest that these crystals correspond to Cr rich oxides and Cr-Mn compounds. Al_2O_3 deposited on untreated SSWC in Fig. 3 (c) was irregularly aggregated in the corners of the channels. Al_2O_3/SSWC in Fig. 3 (c) shows homogeneously deposited Al_2O_3 layer using $Al(NO_3)_3{\cdot}9H_2O$ solution as a precursor, and adhesion of 92 % of the Al_2O_3. The adhesion was increased to 95 % when the SSWC was thermally treated at 800 ℃ for 12 h which can be attributed to the improvement of superficial roughness.

Fig. 4 shows magnified SEM images of Al_2O_3/SSWC800 and Pt/Al_2O_3/SSWC800 by wash-

coat in order to see the morphology and metal compositions on the oxide layer. The SEM images show clearly that the oxide layer (mainly Al_2O_3) was forming cracks on SSWC800, and that the layer has an irregular shape and size. It was thought that this was attributable to the thermal expansion coefficient of the metallic support is different from the oxide layer. After the Pt wash-coat, the oxide layer of Pt/Al_2O_3/SSWC800 had many complex structures which could have contributed to the increased BET surface area (Fig. 1). The EDS sum spectra result for Fig. 4 (a) and Fig. 4 (b) are presented as the composition for Al, Cr, Mn, Fe, Ni, Pt, and O elements in Table 2. From the EDS result, it can be seen that the Pt was detected in Fig. 4 (b), and the Pt particles with 2.67wt% were deposited on Al_2O_3 mixed with oxide layer. However, the particle size of Pt on the metal oxide layer could not be determined from SEM image. For this reason, the crushed Pt/Al_2O_3 layer on SSWC800 was observed by TEM image and result are shown in Fig. 5. Nanosized Pt particles with different sizes could be found in Pt/Al_2O_3, and homogeneous existed in almost below 10 nm. It was also found that the sizes of Pt particles were observed in the range from 2 nm to 8 nm, and an average particle size was 4.5 nm from histogram of particle size (Fig. 5 (b)). Pt loading measured by ICP-AES was 4.3wt%, quite close to the theoretical value (5.0wt%).

3.2. Catalytic activity

Fig. 6 shows the catalytic activity for ethylene oxidation over all the samples as a function of reaction temperatures. Ethylene conversion for untreated SSWC was fairly low starting at 300 ℃ and reaching 54 % of conversion at 500 ℃. It shows clearly that the ethylene oxidation activity was increased by thermal treatment. The higher catalytic activity of SSWC800 may indicate that the oxide layer has an influence on catalytic activity [15,16,31]. However, Al_2O_3/SSWC800 was significantly less active than SSWC800, and that was practically inactive in the reaction temperature range examined. The addition of Pt particles to Al_2O_3/SSWC800 resulted in a significant increase of activity for ethylene oxidation. That is, ethylene conversion over Pt/Al_2O_3/SSWC800 was also increased with increasing reaction temperature and reached to 100 % at ca. 220 ℃. SEM image of Al_2O_3/SSWC800 (Fig. 2 (d)) suggests a better adhesion of the Al_2O_3 to SSWC800 than that to SSWC, which also contributes to improve the catalytic performances because Pt particles can be homogeneously deposited on Al_2O_3/SSWC800. As a

result, catalytic activity for ethylene oxidation showed a positive relationship with the Al_2O_3 adhesion.

Fig. 7 shows the catalytic activity for ethylene oxidation of the Pt/Al_2O_3/SSWC800 and powdered Pt/Al_2O_3 catalyst (GHSV = 2,960 h^{-1}). The Pt/Al_2O_3/SSWC800 reaches complete oxidation in ethylene conversion at over 210 ℃, while the powdered Pt/Al_2O_3 shows 100 % conversion at 170 ℃. The higher catalytic activity of the powdered Pt/Al_2O_3 was considered the influence of the short contact time of the reactant. The Pt/Al_2O_3/SSWC has a lower activity than powdered Pt/Al_2O_3, but the metallic support can minimize the pressure drop associated with high flow rates.

To check the reproducibility, repeated catalytic tests in the range from 150 to 220 □ were performed four times over Pt/Al_2O_3/SSWC800 and were results shown in Fig. 8. It seems to be that the activity is decreased with the increased number of tests, but Pt/Al_2O_3/SSWC800 shows a negligible change of activity in ethylene conversion within the temperature range of ± 5 ℃ during the reproducibility test.

Fig. 9 shows the effect of the GHSV in the range of 1,480 - 8,880 h^{-1} on ethylene conversion which was studied at different temperatures (190 and 210 ℃). As expected, the ethylene conversion is decreased with increased space velocity. For reference, the stability test was performed at 210 ℃ during 92 h with GHSV = 5,920 h^{-1} over Pt/Al_2O_3/SSWC800 in ethylene oxidation activity. It was confirmed that the Pt/Al_2O_3/SSWC800 has a good stability with 35 ± 4.5 % of conversion (data not shown). Finally, the Pt/Al_2O_3/SSWC800 catalyst showed a good reproducibility and stability in ethylene oxidation, which means the SSWC support going through adequate pretreatment process could be known to be an effective support applicable to environmental catalyst system.

4. Conclusions

Here we reported that it is possible to use a stainless steel substrate for catalyst support. Pt/Al_2O_3 catalyst supported on SSWC was prepared and characterized, followed by catalytic activity in ethylene oxidation. When SSWC was pretreated by thermal oxidation, adhesive ability of the Al_2O_3 as primer and superficial roughness were gradually increased. It was also observed

that the deposited Pt particles on Al_2O_3/SSWC by the wash-coat method described were well dispersed with homogeneous size below 10 nm. Pt/Al_2O_3/SSWC has a lower activity than powdered Pt/Al_2O_3, but the supported catalyst can minimize the pressure drop associated with high flow rates. Pt/Al_2O_3/SSWC800 has a good reproducibility and stability in ethylene oxidation, although the ethylene conversion is decreased with increasing space velocity. It has been shown that SSWC is an effective support for environmental catalysts when high flow rates are required.

Acknowledgements

This work was supported by the Korea Research Foundation Grant funded by the Korean Government (MOEHRD, Basic Research Promotion Fund) (KRF-2008-521-D00216). The author also thanks Peter Kreider whose comments greatly improved the final manuscript.

References

[1] R.M. Heck, R.J. Farrauto, S.T. Gulati, *Catalytic air pollution control: Commercial technology*, John Wiley and Sons, New York, 2002, pp. 18-22.

[2] M. Chen, Y. Ma, G. Li, X. Zheng, Catal. Commun. 9 (2008) 990-994.

[3] A. Cybulski, J.A. Moulijn, Catal. Rev.- Sci. Eng. 36 (1994) 179-270.

[4] T.A. Nijhuis, A.E.W. Beers, T. Vergunst, I. Hoek, F. Kapteijn, J.A. Moulijn, Catal. Rev.- Sci. Eng. 43 (2001) 345-380.

[5] J.W. Geus, J.C.van Giezen, Catal. Today 47 (1999) 169-180.

[6] R.M. Heck, R.J. Farrauto, Appl. Catal. A: Gen. 221 (2001) 443-457.

[7] R.M. Heck, S. Gulati, R.J. Farrauto, Chem. Eng. J. 82 (2001) 149-156.

[8] J.P. Reymond, Catal. Today 69 (2001) 343-349.

[9] K.S. Yang, J.S. Choi, S.H. Lee, J.S. Chung, Ind. Eng. Chem. Res. 43 (2004) 907-912.

[10] P. Rodriguez, V. Meille, S. Pallier, M.A.A. Sawah, Appl. Catal. A: Gen. 360 (2009) 154-162.

[11] C.G. Visconti, E. Tronconi, L. Lietti, G. Groppi, P. Forzatti, C. Cristiani, R. Zennaro, S. Rossini, Appl. Catal. A: Gen. 370 (2009) 93-101.

[12] N. Burgos, M. Paulis, M. Antzustegi, M. Montes, Appl. Cat. B: Environ. 38 (2002) 251-258.

[13] O. Sanz, L.M. Martinez T, F.J. Echave, M.I. Dominguez, M.A. Centeno, J.A. Odriozola, M. Montes, Chem. Eng. J. 151 (2009) 324-332.

[14] M. Chen, Y. Ma, G. Li, X. Zheng, Catal. Commun., 9 (2008) 990-994.

[15] L.M. Martinez T, M.I. Dominguez, N. Sanabria, W.Y. Hernandez, S. Moreno, R. Molina, J.A. Odriozola, M.A. Centeno, Appl. Catal. A: Gen. 364 (2009) 166-173.

[16] L.M. Martinez T, D.M. Frias, M.A. Centeno, A. Paul, M. Montes, J.A. Odriozola, Chem. Eng. J. 136 (2008) 390-397.

[17] W. Kaltner, M. Veprek-Heijman, A. Jentys, J.A. Lercher, Appl. Cat. B: Environ. 89 (2009) 123-127.

[18] J.-H. Ryu, K.-Y. Lee, H.-J. Kim, J.-I. Yang, H. Jung, Appl. Cat. B: Environ. 80 (2008) 306-312.

[19] J.M. Zamaro, M.A. Ulla, E.E. Miro, Appl. Catal. A: Gen. 308 (2006) 161-171.

[20] F.N. Aguero, B.P. Barbero, L.C. Almeida, M. Montes, L.E. Cadus, Chem. Eng. J. 166 (2011) 218-223.

[21] B.P. Barbero, L.Costa-Almeida, O. Sanz, M.R. Morales, L.E. Cadus, M. Montes, Chem. Eng. J. 139 (2008) 430-435.

[22] A. Bialas, W. Osuch, W. Lasocha, M. Najbar, Catal. Today 137 (2008) 489-492.

[23] H. Perez, P. Navarro, M. Montes, Chem. Eng. J. 158 (2010) 325-332.

[24] A.F. Ahlström-Silversand and C.U.I. Odenbrand, Chem. Eng. J. 73 (1999) 205-216.

[25] D.Y. Choi, S.J. Kang, K.J. Kim, S.H. Chang, S.I. Boo, W.J. Jeong, B.K. Son, H.G. Ahn, J. Korean Soc. Environ. Technol. 10 (2009) 193-200.

[26] K.J. Kim, H.G. Ahn, Appl. Catal. B.: Environ. 91 (2009) 308-318.

[27] JCPDS Powder Diffraction File, International Centre for Diffraction Data, Swarthmore, PA, 1991.

[28] G. Bergeret, P. Gallezot, Handbook of Heterogeneous Catalysis; G. Ertl, H. Knozinger, J. Weitkamp, Ed., VCH, Weinheim, 1997, pp. 439-462.

[29] L.M. Martinez T, O. Sanz, M.I. Dominguez, M.A. Centeno, J.A. Odriozola, Chem. Eng. J. 148 (2009) 191-200.

[30] S. Brunauer, L.S. Deming, W.E. Deming, E. Teller, J. Am. Chem. Soc. 62 (1940) 1723-1732.

[31] M.I. Dominguez, M. Sanchez, M.A. Centeno, M. Montes, J.A. Odriozola, Appl. Catal. A:

Gen. 302 (2006) 96-103.

Tables

Table 1. Textural properties of SSWC, SSWC800, Al_2O_3/SSWC800, and Pt/Al_2O_3/SSWC800

Samples	S_{BET} (m^2/g)[a]	V_{total} (10^{-3} cm^3/g)[b]	$D_{average}$ (nm)[c]
SSWC	2.6 ± 0.08	0.1	2.1
SSWC800	4.0 ± 0.13	2.2	2.6
Al_2O_3/SSWC800	16.9 ± 0.21	14.1	2.5
Pt/Al_2O_3/SSWC800	17.0 ± 0.18	14.4	2.5

[a]BET surface area, based on the linear part of the 5 point adsorption data at P/P_0 = 0.06 - 0.20.

[b]Total pore volume, calculated by the HK method at P/P_0 = 0.97.

[c]Average pore diameter, caculated by the HK method at P/P_0 = 0.01 - 0.70.

Table 2. EDS sum spectra analysis for Fig. 4 (a) and Fig. 4 (b)

Elements	Composition (wt%)	
	Fig. 4 (a)	Fig. 4 (b)
Al	6.68	19.87
Cr	34.02	24.23
Mn	10.78	7.83
Fe	21.51	23.76
Ni	3.66	-
Pt	-	2.67
O	23.34	21.64

Figure captions

Fig. 1. N_2 adsorption isotherms of SSWC, SSWC800, Al_2O_3/SSWC800, and Pt/Al_2O_3/SSWC800.

Fig. 2. XRD patterns of SSWC (a), SSWC800 (b), Al_2O_3/SSWC800 (c), and Pt/Al_2O_3/SSWC800 (d).

Fig. 3. SEM images of SSWC (a), SSWC800 (b), Al_2O_3/SSWC (c), and Al_2O_3/SSWC800 (d).

Fig. 4. SEM images of Al_2O_3/SSWC800 (a) and Pt/Al_2O_3/SSWC800 (b).

Fig. 5. STEM image (a) and histogram of particle size (b) of Pt/Al_2O_3/SSWC800.

Fig. 6. Effect of reaction temperature on catalytic activity for ethylene oxidation (GHSV = 5,920 h^{-1}).

Fig. 7. Comparisons of catalytic activity for ethylene oxidation between the powdered Pt/Al_2O_3 and Pt/Al_2O_3/SSWC800 (GHSV = 2,960 h^{-1}).

Fig. 8. Reproducibility test on catalytic activity for ethylene oxidation over Pt/Al_2O_3/SSWC800 (GHSV = 5,920 h^{-1}).

Fig. 9. Effect of GHSV on ethylene conversion over Pt/Al_2O_3/SSWC800 at different temperatures.

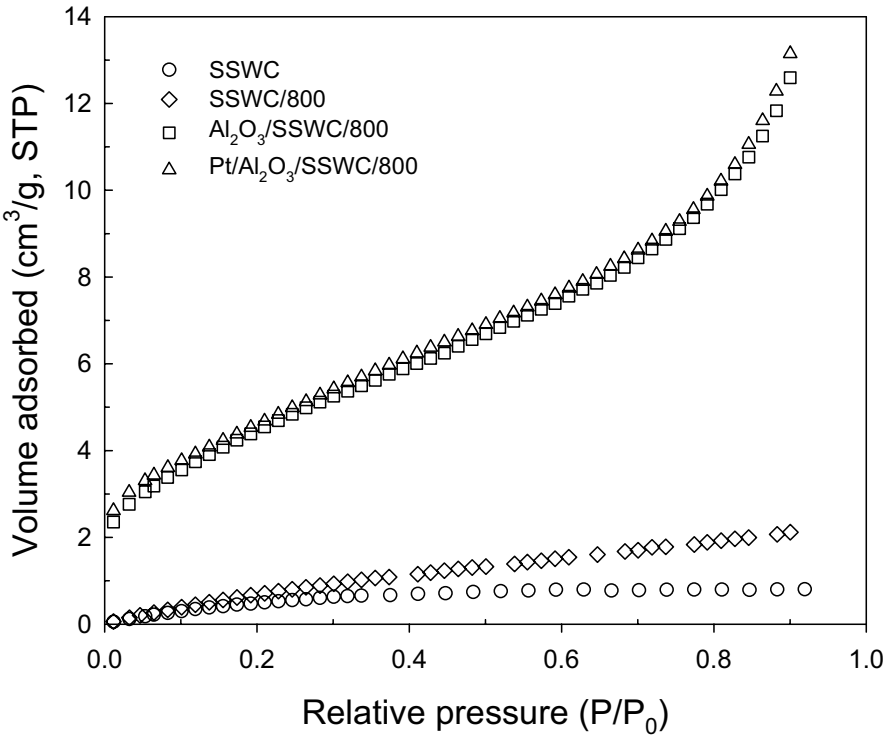

Fig. 1. N_2 adsorption isotherms of SSWC, SSWC800, Al_2O_3/SSWC800, and Pt/Al_2O_3/SSWC800.

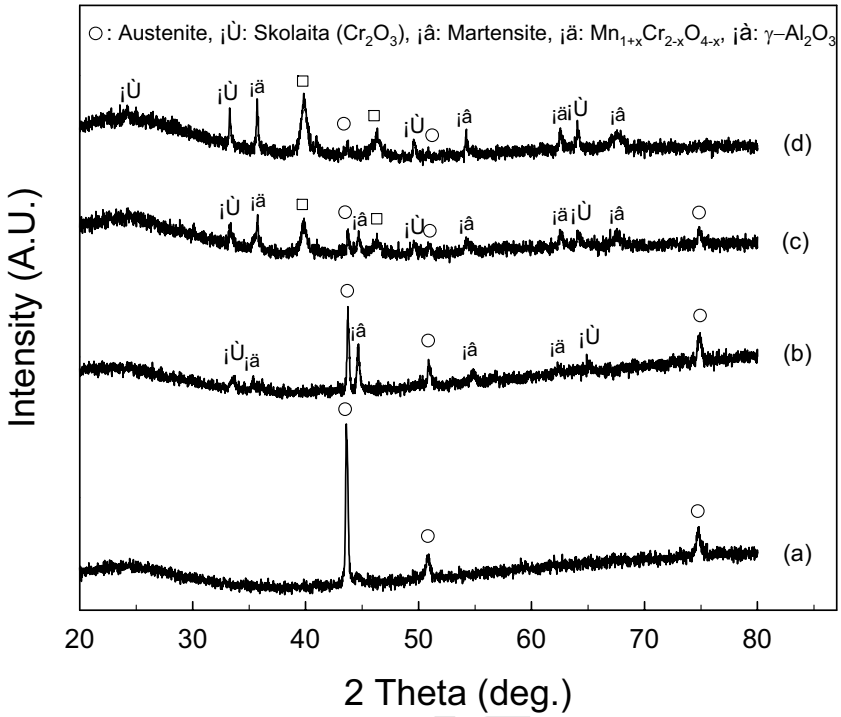

Fig. 2. XRD patterns of SSWC (a), SSWC800 (b), Al_2O_3/SSWC800 (c), and Pt/Al_2O_3/SSWC800 (d).

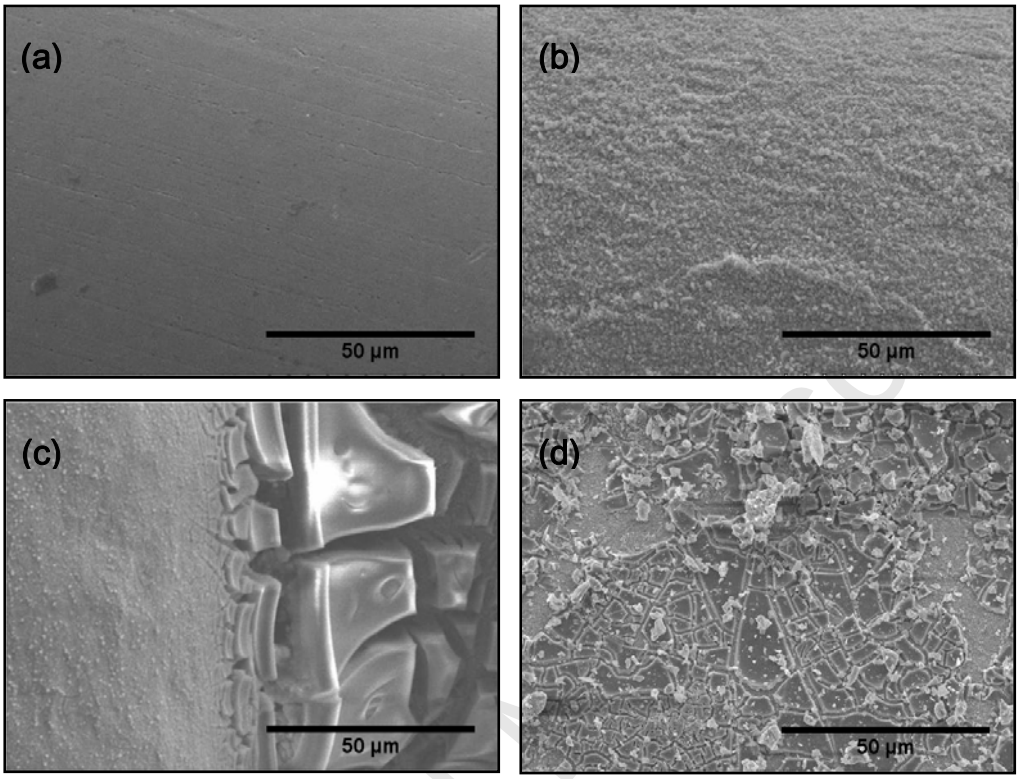

Fig. 3. SEM images of SSWC (a), SSWC800 (b), Al_2O_3/SSWC (c), and Al_2O_3/SSWC800 (d).

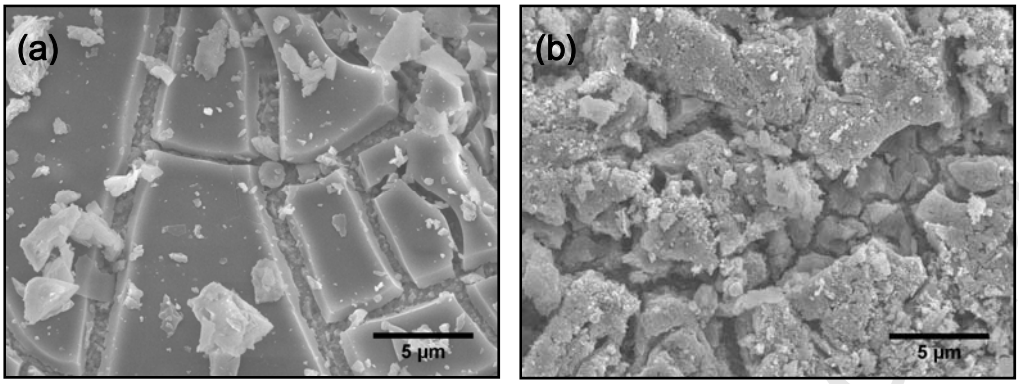

Fig. 4. SEM images of Al_2O_3/SSWC800 (a) and Pt/Al_2O_3/SSWC800 (b).

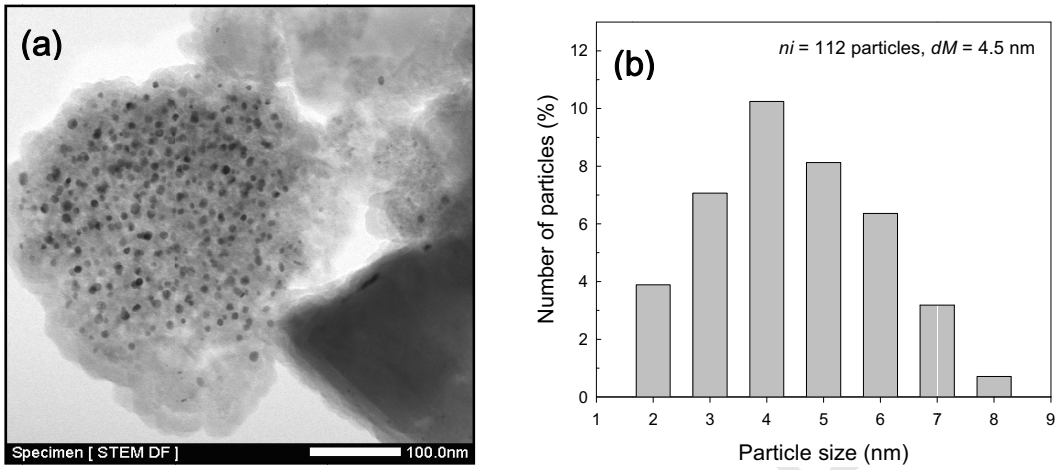

Fig. 5. STEM image (a) and histogram of particle size (b) of Pt/Al_2O_3/SSWC800.

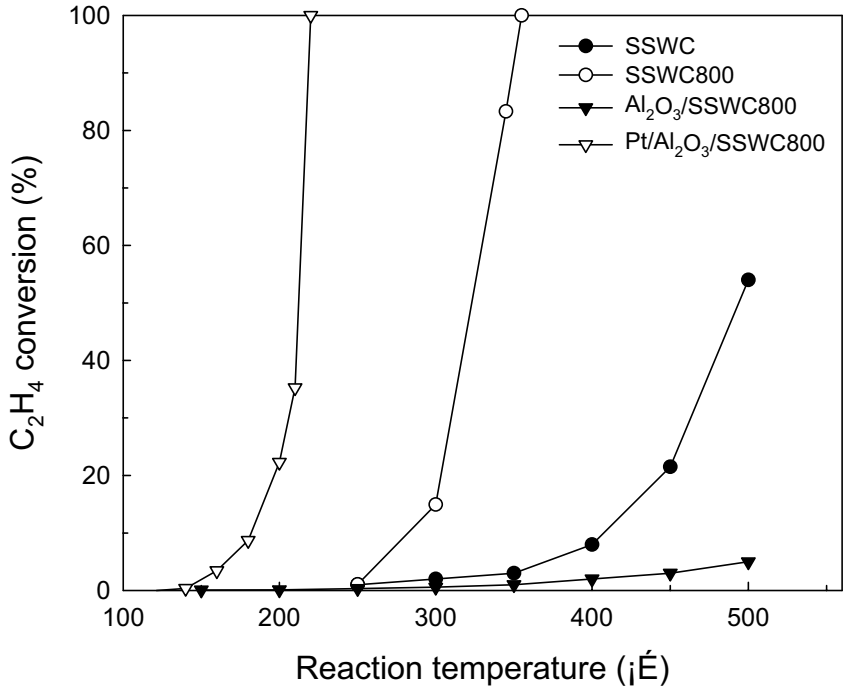

Fig. 6. Effect of reaction temperature on catalytic activity for ethylene oxidation (GHSV = 5,920 h^{-1}).

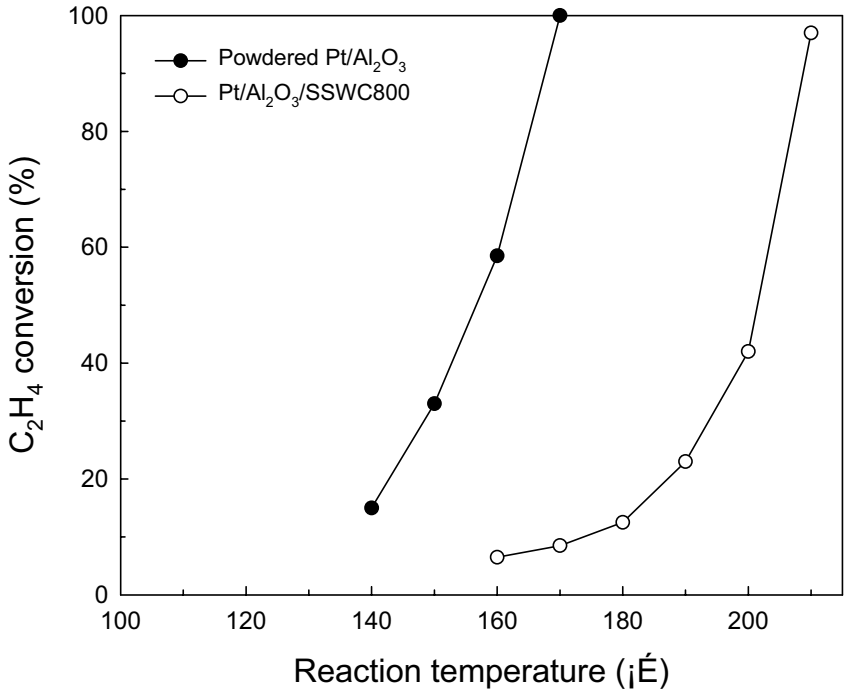

Fig. 7. Comparisons of catalytic activity for ethylene oxidation between the powdered Pt/Al_2O_3 and Pt/Al_2O_3/SSWC800 (GHSV = 2,960 h^{-1}).

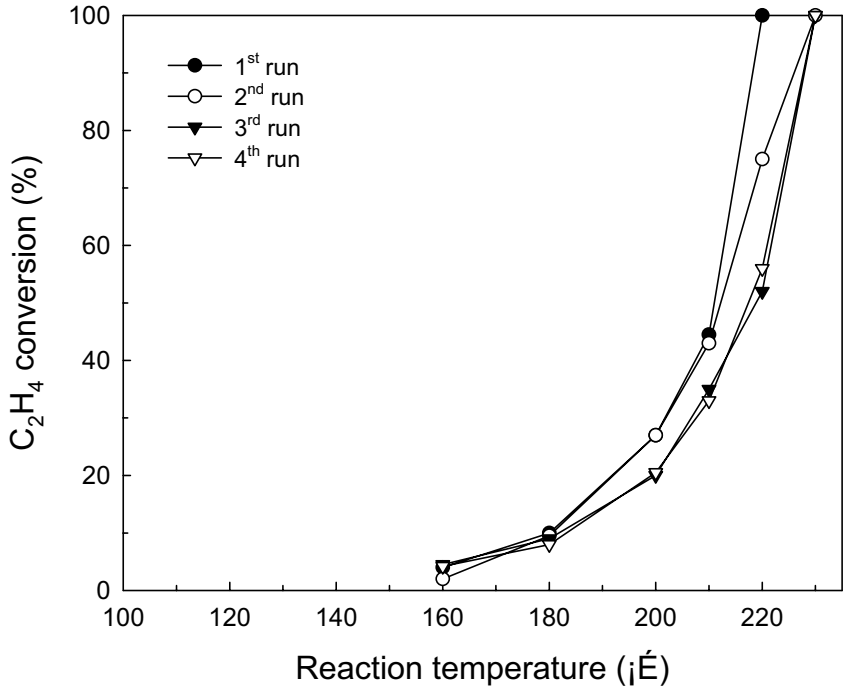

Fig. 8. Reproducibility test on catalytic activity for ethylene oxidation over $Pt/Al_2O_3/SSWC800$ (GHSV = 5,920 h^{-1}).

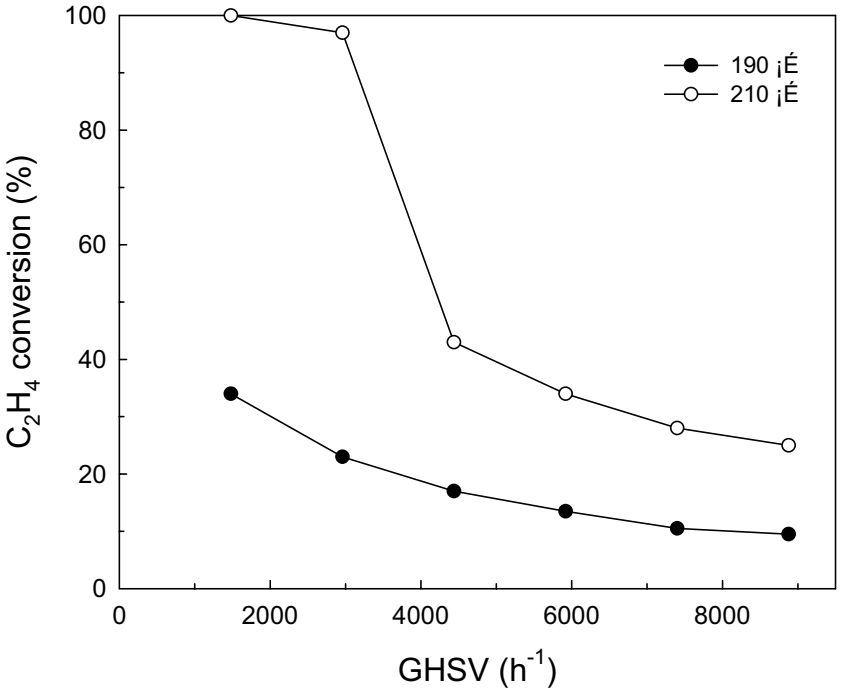

Fig. 9. Effect of GHSV on ethylene conversion over $Pt/Al_2O_3/SSWC800$ at different temperatures.